Supporting Information for

Three-dimensional porphyrin-based covalent organic frameworks with tetrahedral building blocks for single-site catalysis

Yong Liu,‡[a] Xiao-dong Yan,‡[a] Tao Li,[a] Wen-Da Zhang,[a] Qiu-Ting Fu,[a] Hui-Shu Lu,[a] Xuan Wang,[a] and Zhi-Guo Gu[*a,b]*

a. Key Laboratory of Synthetic and Biological Colloids, Ministry of Education, School of Chemical and Material Engineering, Jiangnan University, Wuxi 214122, P.R. China. E-mail: zhiguogu@jiangnan.edu.cn.
b. International Joint Research Center for Photoresponsive Molecules and Materials, School of Chemical and Material Engineering, Jiangnan University, Wuxi 214122, P.R. China.
‡ These authors contributed equally.

E-mail: zhiguogu@jiangnan.edu.cn

Contents

1. General information

^{1}H NMR (400 MHz) and ^{13}C NMR (101 MHz) spectra were recorded in Dimethyl sulfoxide-d6 at room temperature on a Bruker using TMS as the internal reference. Fourier transform infrared (FT-IR) spectra were recorded on a NICOLET 6700 FTIR Spectrometer. Solid-state ^{13}C cross-polarization magic-angle spinning (CP/MAS) NMR measurement was performed with a Bruker AVANCE III 500 spectrometer. UV-Vis absorbance spectra were collected on UV-3600 Plus UV-VIS-NIR spectrophotometer. Scanning Electron Microscopy (SEM, HitachiS-4800) accompanied by Energy dispersive X-ray spectrometry (EDX; accelerated voltage: 20 kV) was used to further study the morphology and the elements distribution of the samples. The X-ray photoelectron spectra (XPS) were carried out by Multifunctional imaging electron spectrometer (Thermo ESCALAB 250XI), from which can analyze the composition of elements. The inductively coupled plasma (ICP) measurements were recorded on a Leeman lab, inc. Profile Plus high dispersion ICP. UV-Vis-IR diffuse reflectance spectrum (Kubelka-Munk spectrum) was recorded on a JASCO model V-670 spectrometer equipped with integration sphere model IJN-727. Powder electrical conductivity was recorded on a Suzhou Jingge ST2253 by four-probe method. The nitrogen sorption isotherms and pore-size distribution curves were measured at the temperature of liquid nitrogen (77 K) by using an automatic volumetric adsorption equipment (Mircomeritics, ASAP2010). Thermal gravimetric analysis (TGA) measurement was performed on a TGA/1100SF thermo grabinetric analyzer. Transmission electron microscopy (TEM) images were obtained on a JEOL model JEM-2100 microscope to further study the morphology. Powder X-ray diffraction (PXRD) dates were collected on a D 8 Advance X-ray diffractometer (Bruker AXS Germany) with Cu Kα radiation at 40 kV 200 mA with scanning rate of $2°\cdot min^{-1}$ (2θ) at room temperature. The crystal structures were determined on a Siemens (Bruker) SMART CCD diffractometer using monochromated Mo $K\alpha$ radiation (λ = 0.71073 Å). Cell parameters were retrieved using SMART software and

refined using SAINT on all observed reflections.[1] The highly redundant data sets were reduced using SAINT and corrected for Lorentz and polarization effects. Absorption corrections were applied using SADABS supplied by Bruker.[2] Structures were solved by direct methods using the program SHELXL-2014/7.[3] In model compound MC, the unit cell includes some disordered solvent molecules, which could not be modeled as discrete atomic sites. Accordingly, the SQUEEZE[4] function of PLATON[5] was employed to remove this contribution from the model. The formula and parameters in Table S4 do not include solvent.

2. The synthesis and characterization of 3,3',5,5'-tetrakis(4-formylphenyl)bimesityl (TFBM)

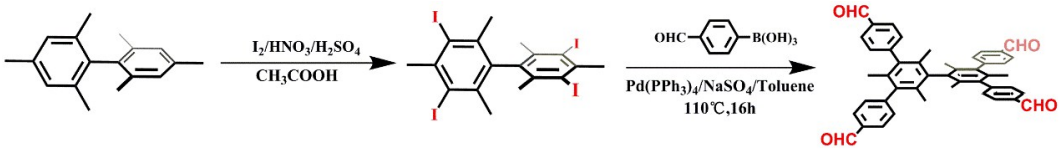

BM TIBM TFBM

TFBM was synthesized according to a previous method with slight modification.[6] To a 100 mL round bottom flask, bimesityl (4.76 g, 20.0 mmol) in 2.5 mL of $CHCl_3$ and 12 mL of CH_3COOH, and iodine (11.18 g, 44 mmol) were added under nitrogen atmosphere. Then HNO_3 (19 mL) and H_2SO_4 (19 mL) were added to the solution with stirring at room temperature. After stirring for 3 h, the mixture was poured into ice, washed with 2M NaOH and saturated $Na_2S_2O_3$ solution. The resultant precipitate was filtered and recrystallized from ethyl acetat to obtain 3,3',5,5'-tetraiodobimesityl (12 g, 80 %). In a 120 mL pressure tube, 3,3',5,5'-tetraiodobimesityl (0.742 g, 1 mmol) was dispersed in 20 mL of toluene and 20 mL of saturated $NaHCO_3$ solution, and then 4-formylphenylboronic acid (1.51 g, 10 mmol) and $Pd(PPh_3)_4$ (0.576 g, 0.5 mmol) were added under nitrogen atmosphere. The reaction mixture was heated at 110 °C for 16 h, and the yellow turbid solution turned to dark brown. The mixture was cooled down to room temperature and extracted with ethyl acetate (3 × 20 mL). The extracts were washed with deionized water and dried over saturated Na_2SO_4.The product was purified by column chromatography with silica gel using ethyl acetate and petroleum ether mixture (5:95) as an eluent, and dried by vacuum oven to obtain white solid of TFBM. Yield: 20 %. Anal. Calcd (%) for $C_{46}H_{38}O_4$: C, 84.38; H, 5.85; O, 9.77. Found: C, 84.34; H, 5.86; N, 9.80; ATR-FTIR cm^{-1}: 3042, 1691, 1602; ^1H NMR (CDCl3, 400MHz, δ/ppm) δ 1.70 (s, 6H), 1.71 (s, 12 H), 7.41 (d, 8H), 7.98 (d, 8H), 10.10 (s, 4H); ^{13}C NMR (100 MHz, $CDCl_3$) δ 18.33, 19.23, 130.06, 130.28, 131.46, 132.62, 135.07, 138.56, 139.34, 148.72, 191.97; MS (EI) m/z: 655 M^+.

The single crystals of TFBM were grown by a solution diffusion method. In a 15 mL test tube, a mixture of dichloromethane and methanol (v/v, 1:1, 4 mL) was gently

layered on the top of a 3 mL dichloromethane solution of TFBM (30 mg, 0.046 mmol), and then 4 mL methanol was added carefully as a third layer. After two weeks, colorless crystals were collected, then washed with H_2O and dried in atmosphere.

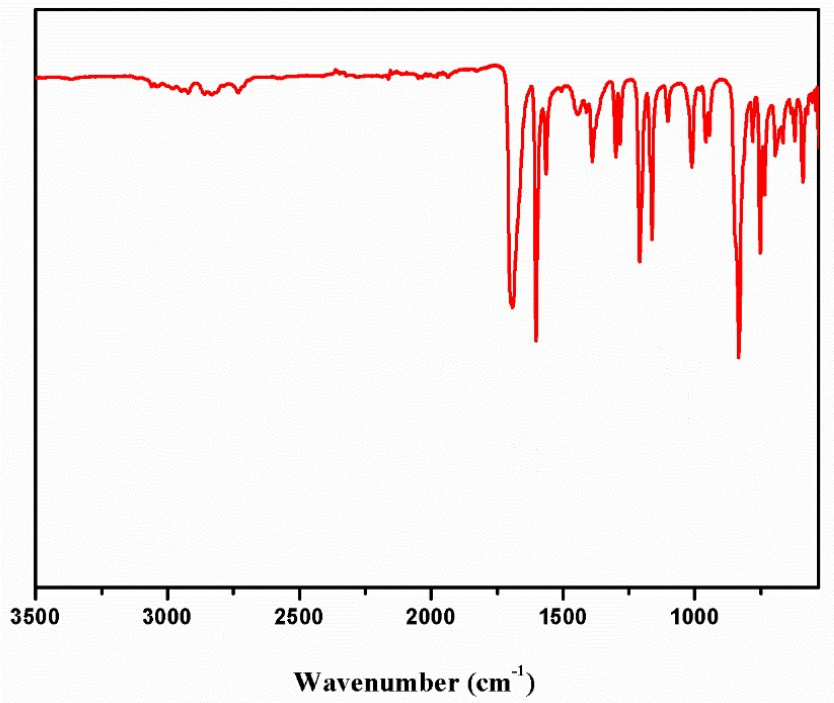

Fig. S1 The ATR-FTIR spectrum of TFBM.

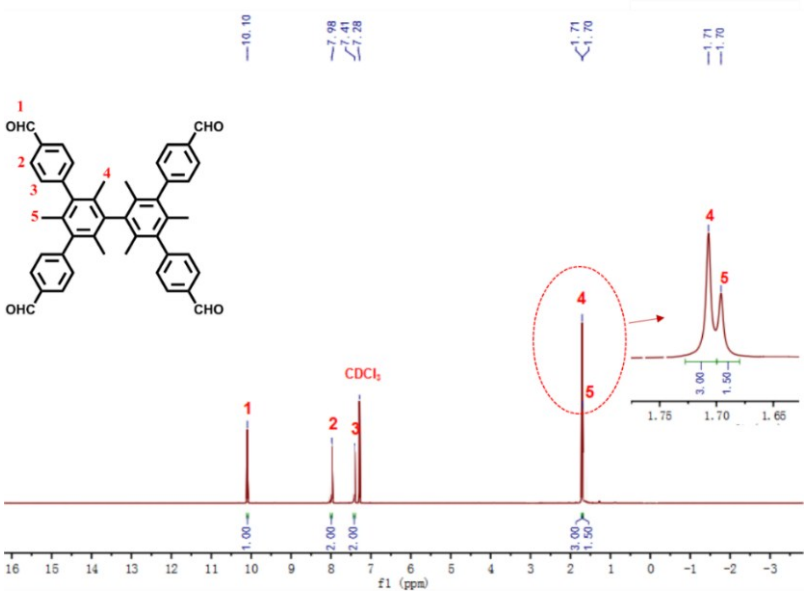

Fig. S2 The ^{1}H NMR spectrum of TFBM.

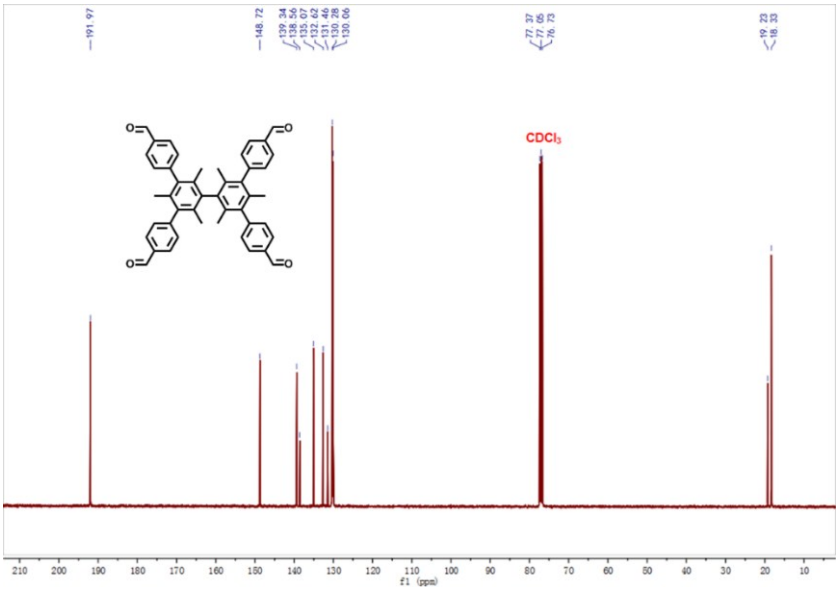

Fig. S3 The ^{13}C NMR spectrum of TFBM.

3. The synthesis and characterization of 5, 10, 15, 20-tetra(4-aminophenyl)porphyrin (TAPP)

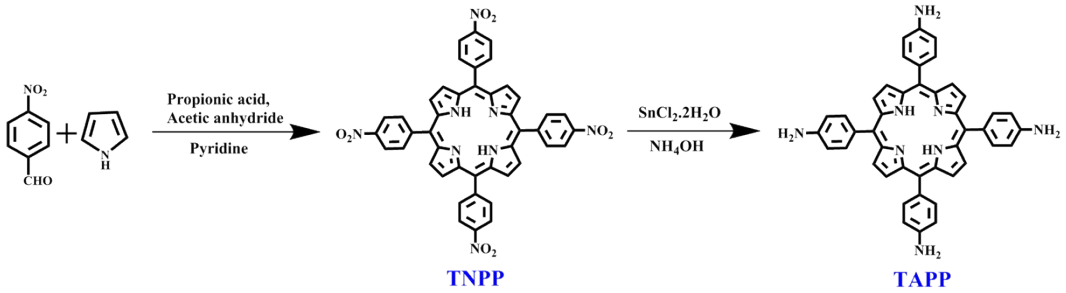

TAPP was synthesized according to previous methods with slight adjustment.[7] The pure product TAPP was finally isolated as purple powder. Yield: 23 %. Anal. Calcd (%) for $C_{44}H_{34}N_8$: C, 78.32; H, 5.08; N, 16.60. Found: C, 78.29; H, 5.09; N, 16.62; ATR-FTIR cm^{-1}: 3336, 1623, 1517, 1453, 1335, 1273, 1171, 955, 811, 741, 532; ^1H NMR (DMSO, 400 MHz, δ/ppm): -2.7 (s, 2H), 5.58 (s, 8H), 7.01(d, 8H), 7.86(d, 8H), 8.89 (s, 8H); ^{13}C NMR (101 MHz, DMSO, δ ppm): 148.98, 135.92, 129.20, 121.04, 112.98; MS (EI) m/z: 674 M^+.

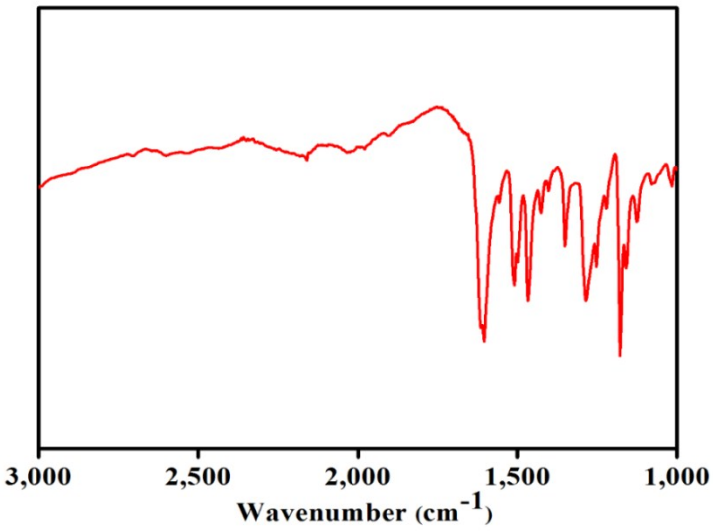

Fig. S4 The ATR-FTIR spectrum of TAPP.

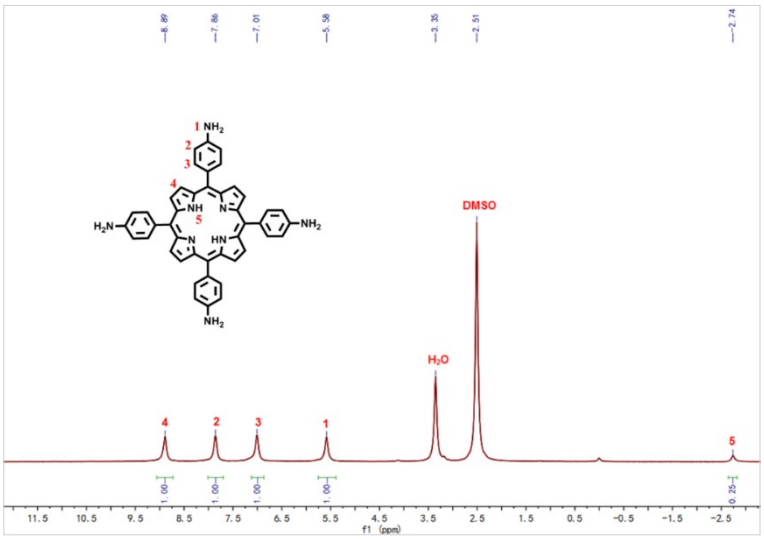

Fig. S5 The ^{1}H NMR spectrum of TAPP.

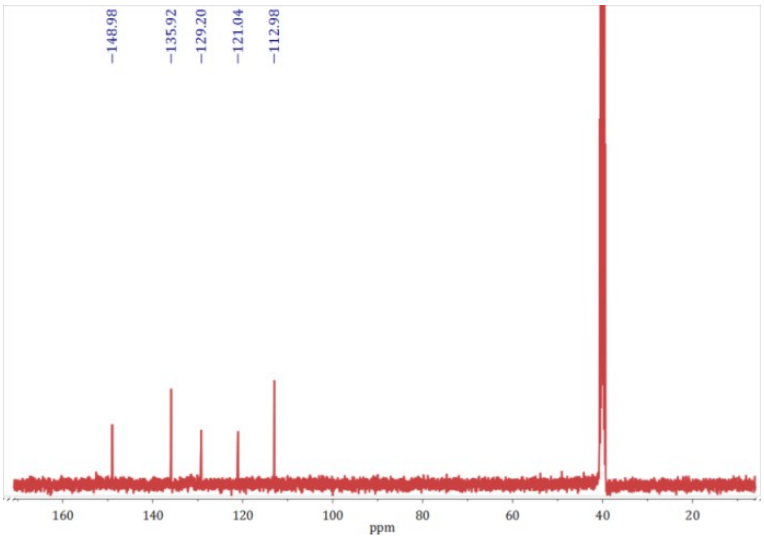

Fig. S6 The ^{13}C NMR spectrum of TAPP.

4. The synthesis and characterization of 5, 10, 15, 20-tetra(4-aminobiphenyl)porphyrin (TABPP)

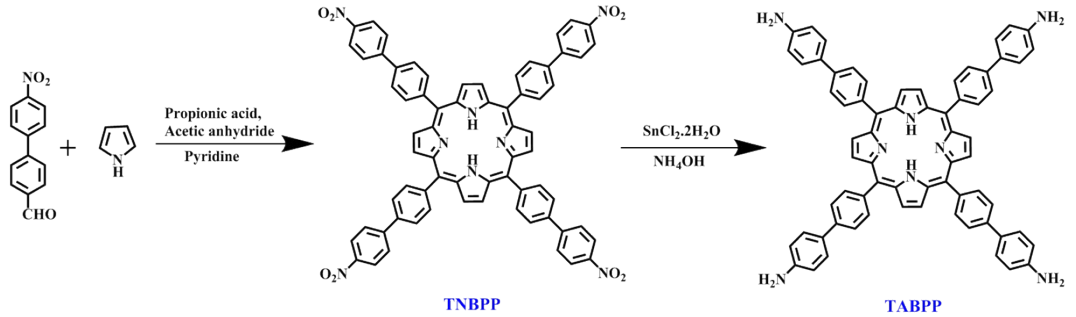

TABPP was synthesized using 4′-nitrobiphenyl-4-carbaldehyde (15 g, 66 mmol) following the procedures used for the preparation of TAPP. The pure product TABPP was finally isolated as purple powder.[8] Yield: 20 %. Anal. Calcd (%) for $C_{68}H_{50}N_8$: C, 83.41; H, 5.15; N, 11.44. Found: C, 83.43; H, 5.12; N, 11.45; ATR-FTIR cm^{-1}: 3366, 3216, 1618, 1499; ^1H NMR (DMSO, 400 MHz, δ/ppm): -2.81 (s, 2H), 5.39 (s, 8H), 6.78 (d, 8H), 7.71(d, 8H), 7.98(d, 8H), 8.18 (d, 8H), 8.92 (s, 8H); ^{13}C NMR (101 MHz, DMSO, δ ppm): 149.25, 140.54, 138.94, 135.30, 127.96, 127.13, 124.19, 120.41, 114.93; MS (EI) m/z: 978.42 M^+.

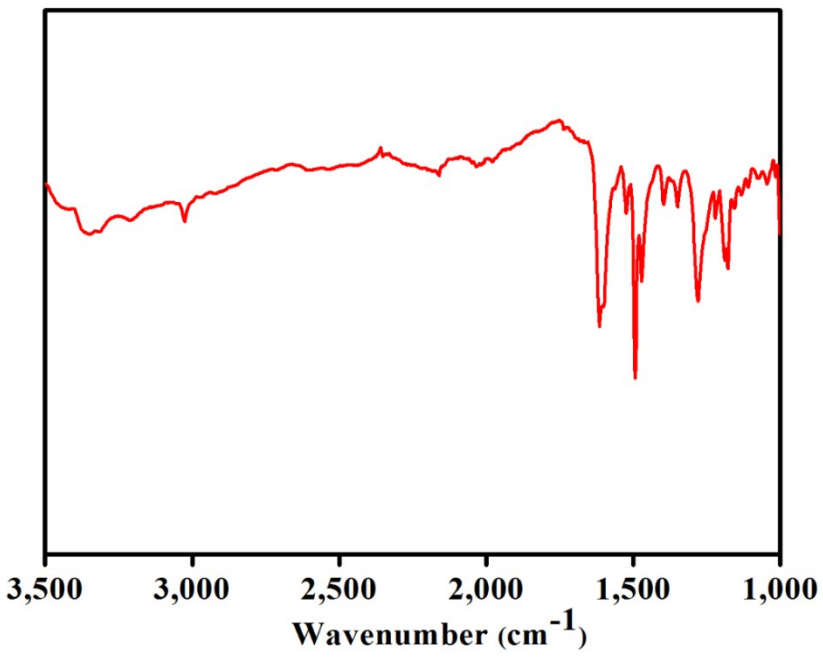

Fig. S7 The ATR-FTIR spectrum of TABPP.

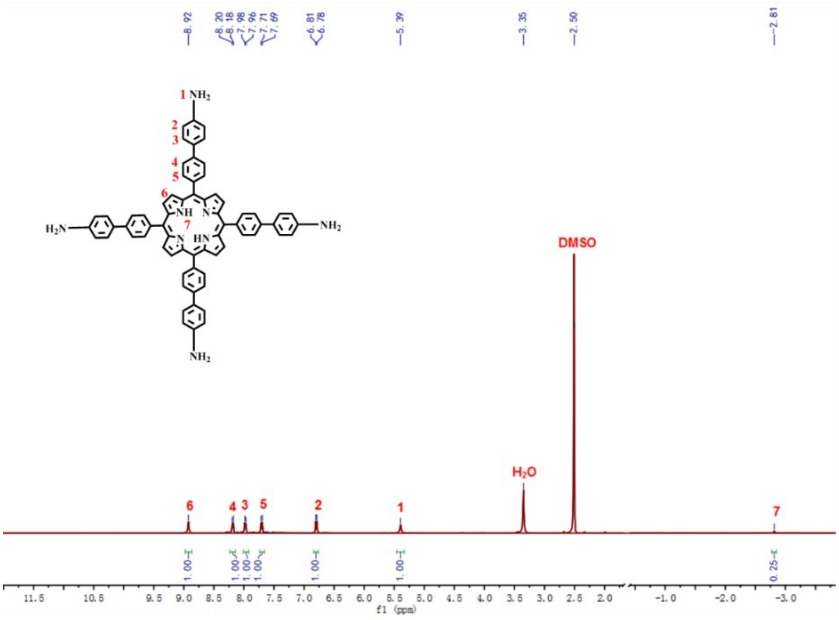

Fig. S8 The ^{1}H NMR spectrum of TABPP.

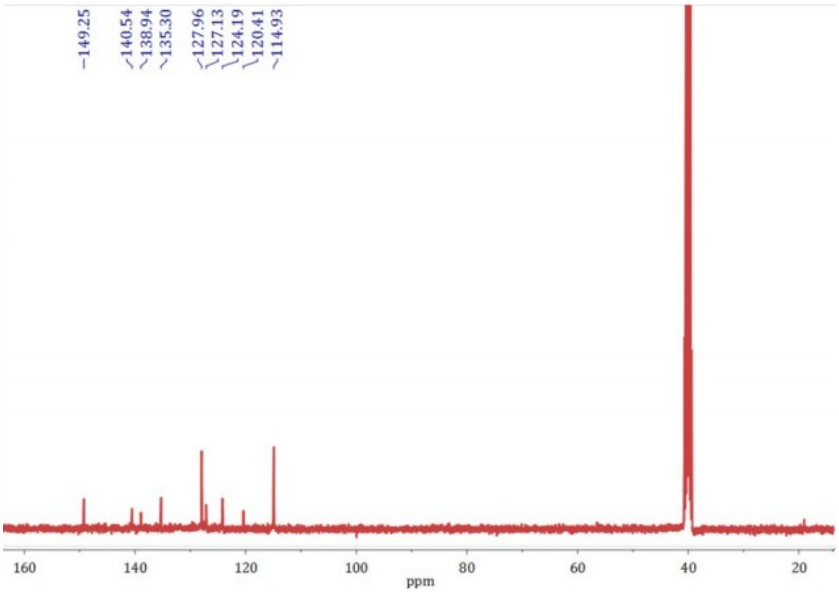

Fig. S9 The ^{13}C NMR spectrum of TABPP.

5. The synthesis and characterization of MC

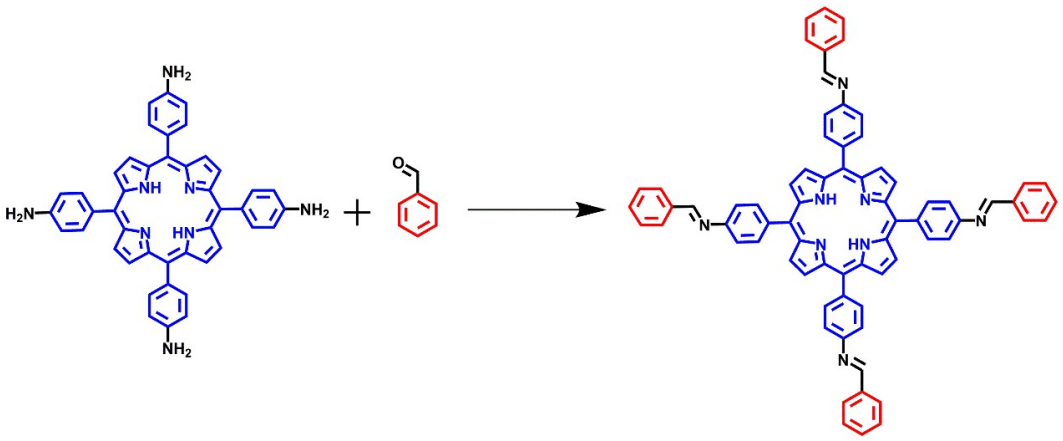

Model Compound

In a 25 mL round bottom flask, TAPP (67 mg, 0.1 mmol) and benzaldehyde (42 mg, 0.4 mmol) was dissolved in chloroform (10 mL) under nitrogen atmosphere. The mixture was refluxed for 6 h, then cooled to room temperature and filtered to obtain purple solution. The product was separated out by adding the absolute methanol (20 mL) in the purple solution, filtered and dried by vacuum oven to obtain purple solid of MC. Anal. Calcd (%) for $C_{72}H_{50}N_8$: C, 84.19; H, 4.91; N, 10.90. Found: C, 84.15; H, 4.93; N, 10.92; ATR-FTIR cm^{-1}: 3314, 3024, 1629, 1594, 1167; ^{1}H-NMR ($CDCl_3$, 300 MHz, δ/ppm): -2.66 (s, 2H), 7.60 (t, 12H), 7.65 (d, 8H), 8.8.11 (m, 8H), 8.28 (d, 8H), 8.87 (s, 4H), 8.98 (s, 8H). MS (EI) m/z: 1027.42 M^+.

The single crystals of MC were grown by a solution diffusion method. In a 20 mL test tube, a mixture of chloroform and methanol (v/v, 1:1, 5 mL) was gently layered on the top of a 3 mL purple solution and then 5 mL methanol was added carefully as a third layer. After three weeks, purple needle-like crystals of MC were collected, then washed with H_2O and dried in atmosphere.

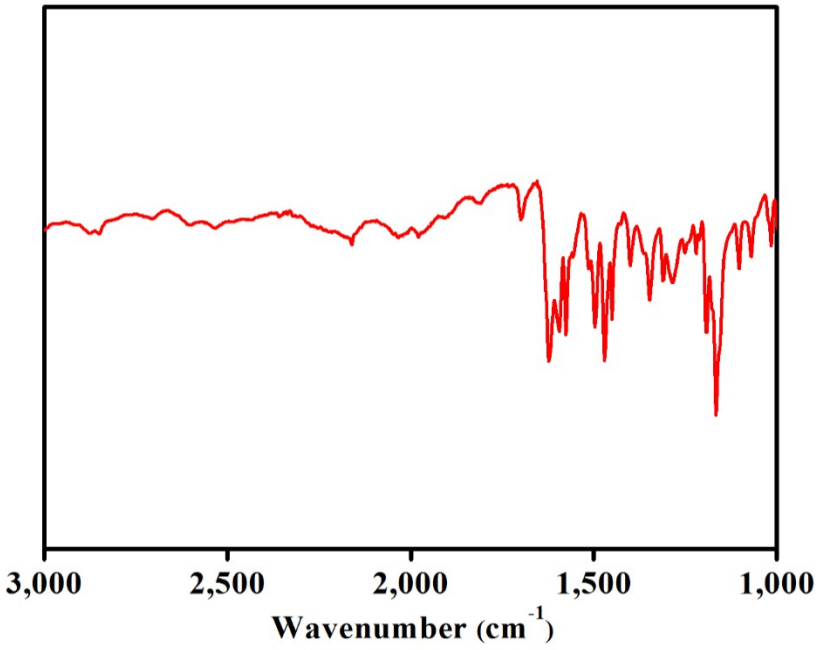

Fig. S10 The ATR-FTIR spectrum of MC.

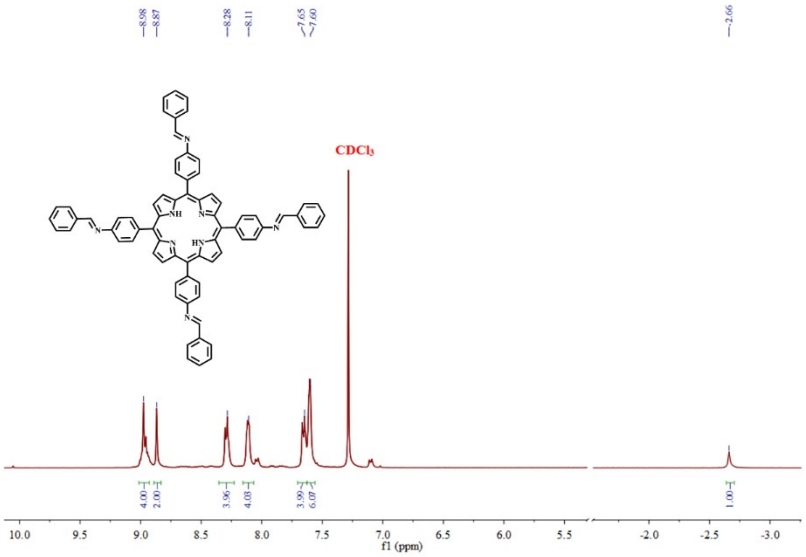

Fig. S11 The ^{1}H NMR spectrum of MC.

6. The characterization of PCOF, PCOF-Fe and PCOF-Co

Table S1. Reaction conditions screening with different solvents system for the synthesis of PCOF-1.

Entry	Solvents	T (°C)	Catalyst	Crystallinity
PCOF-1 (1)	Dioxane/Mesitylene = 1/1	120	6 M Acetic acid	No
PCOF-1 (2)	Dioxane/Mesitylene = 0.5/1.5	120	6 M Acetic acid	No
PCOF-1 (3)	Dioxane/Mesitylene = 1.5/0.5	120	6 M Acetic acid	No
PCOF-1 (4)	o-dichlorobenzene/n-butanol = 1/1	120	6 M Acetic acid	Low
PCOF-1 (5)	o-dichlorobenzene/n-butanol = 0.5/1.5	120	6 M Acetic acid	No
PCOF-1 (6)	o-dichlorobenzene/n-butanol = 1.5/0.5	120	6 M Acetic acid	Moderate
PCOF-1 (7)	o-dichlorobenzene/n-butanol = 1.5/0.5	150	6 M Acetic acid	Low
PCOF-1 (8)	o-dichlorobenzene/n-butanol = 1.5/0.5	120	3 M Acetic acid	Low
PCOF-1 (9)	o-dichlorobenzene/Mesitylene = 1/1	120	6 M Acetic acid	Moderate
PCOF-1 (10)	o-dichlorobenzene/Mesitylene = 1.5/0.5	120	6 M Acetic acid	High
PCOF-1 (11)	o-dichlorobenzene/Mesitylene = 1.7/0.3	120	6 M Acetic acid	High

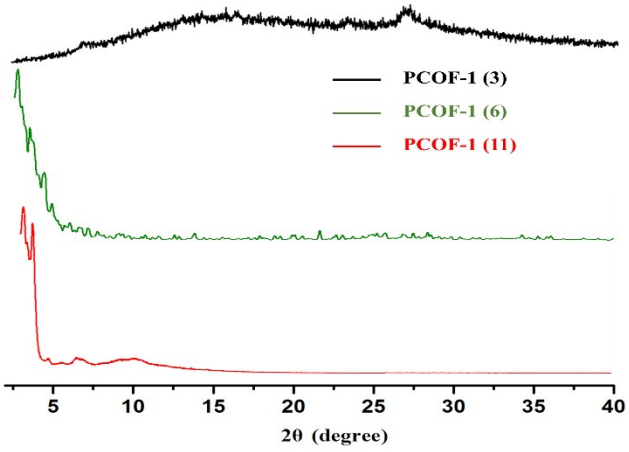

Fig. S11 PXRD of different samples of **PCOF-1** (optimization entries 3, 6 and 11 in Table S1).

Table S2. Reaction conditions screening with different solvents system for the synthesis of PCOF-2.

Entry	Solvents	T (°C)	Catalyst	Crystallinity
PCOF-2 (1)	Dioxane/Mesitylene = 1/1	120	6 M Acetic acid	No
PCOF-2 (2)	Dioxane/Mesitylene = 0.5/1.5	120	6 M Acetic acid	No
PCOF-2 (3)	Dioxane/Mesitylene = 1.5/0.5	120	6 M Acetic acid	No
PCOF-2 (4)	o-dichlorobenzene/n-butanol = 1/1	120	6 M Acetic acid	No
PCOF-2 (5)	o-dichlorobenzene/n-butanol = 0.5/1.5	120	6 M Acetic acid	No
PCOF-2 (6)	o-dichlorobenzene/n-butanol = 1.5/0.5	120	6 M Acetic acid	Moderate
PCOF-2 (7)	o-dichlorobenzene/n-butanol = 1.5/0.5	150	6 M Acetic acid	Low
PCOF-2 (8)	o-dichlorobenzene/n-butanol = 1.5/0.5	120	3 M Acetic acid	No
PCOF-2 (9)	o-dichlorobenzene/Mesitylene = 1/1	120	6 M Acetic acid	Low
PCOF-2 (10)	o-dichlorobenzene/Mesitylene = 1.5/0.5	120	6 M Acetic acid	Moderate
PCOF-2 (11)	o-dichlorobenzene/Mesitylene = 1.7/0.3	120	6 M Acetic acid	High

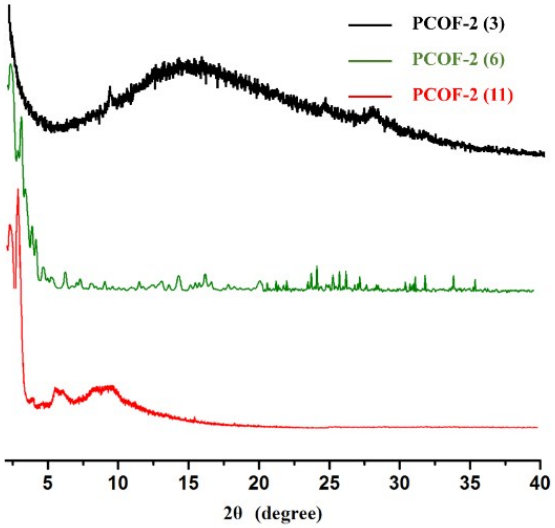

Fig. S12 PXRD of different samples of **PCOF-2** (optimization entries 3, 6 and 11 in Table S2).

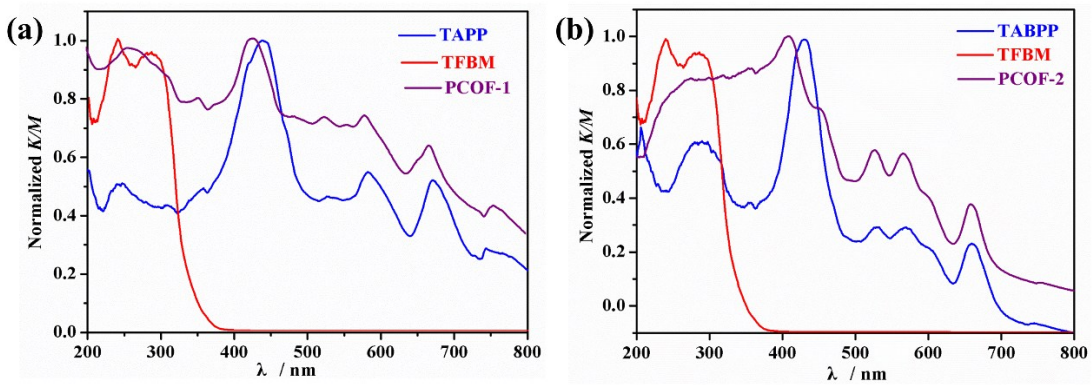

Fig. S13 Kubelka–Munk function for diffuse reflectance spectra of (a) TAPP, TFBM and **PCOF-1**; (b) TABPP, TFBM and **PCOF-2**. Spectra are normalized to global absorption maximum.

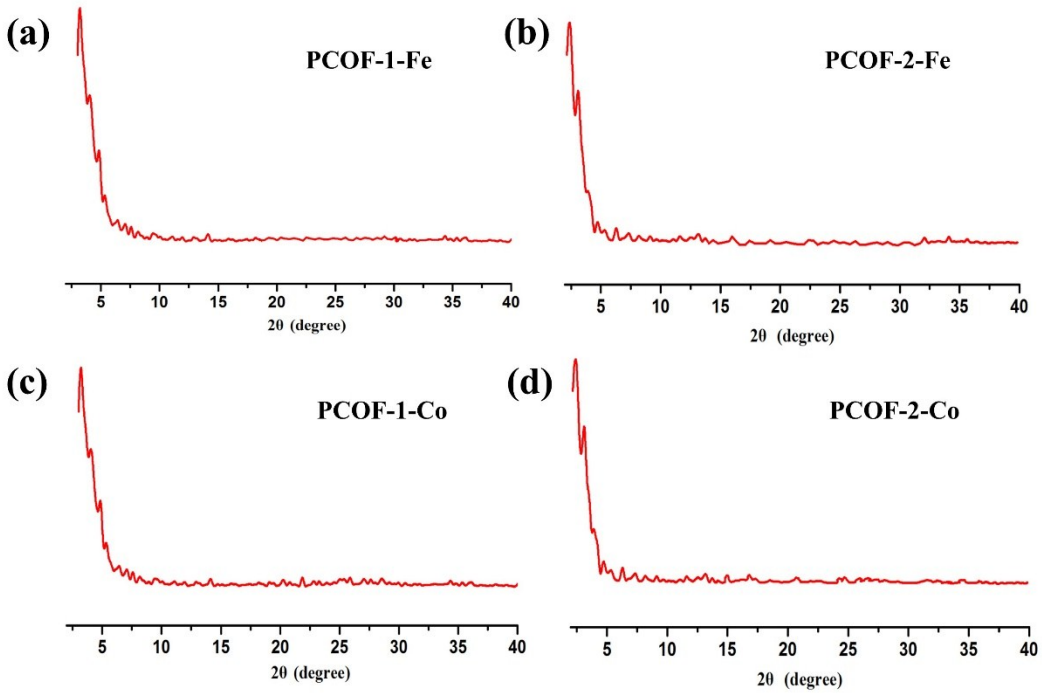

Fig. S14 PXRD patterns of (a) **PCOF-1-Fe**, (b) **PCOF-2-Fe**, (c) **PCOF-1-Co** and (d) **PCOF-2-Co**.

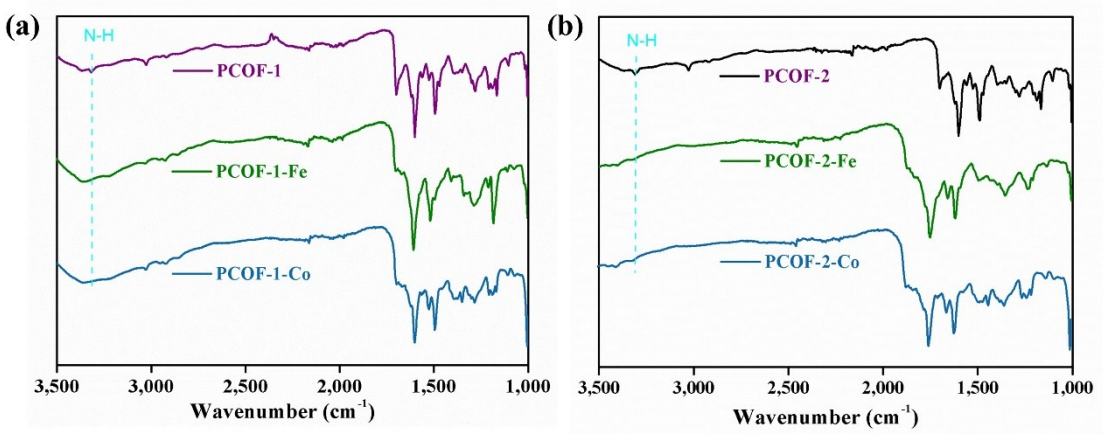

Fig. S15 The ATR-FTIR spectrum of (a) **PCOF-1**, **PCOF-1-Fe** and **PCOF-1-Co**; (b) **PCOF-2**, **PCOF-2-Fe** and **PCOF-2-Co**.

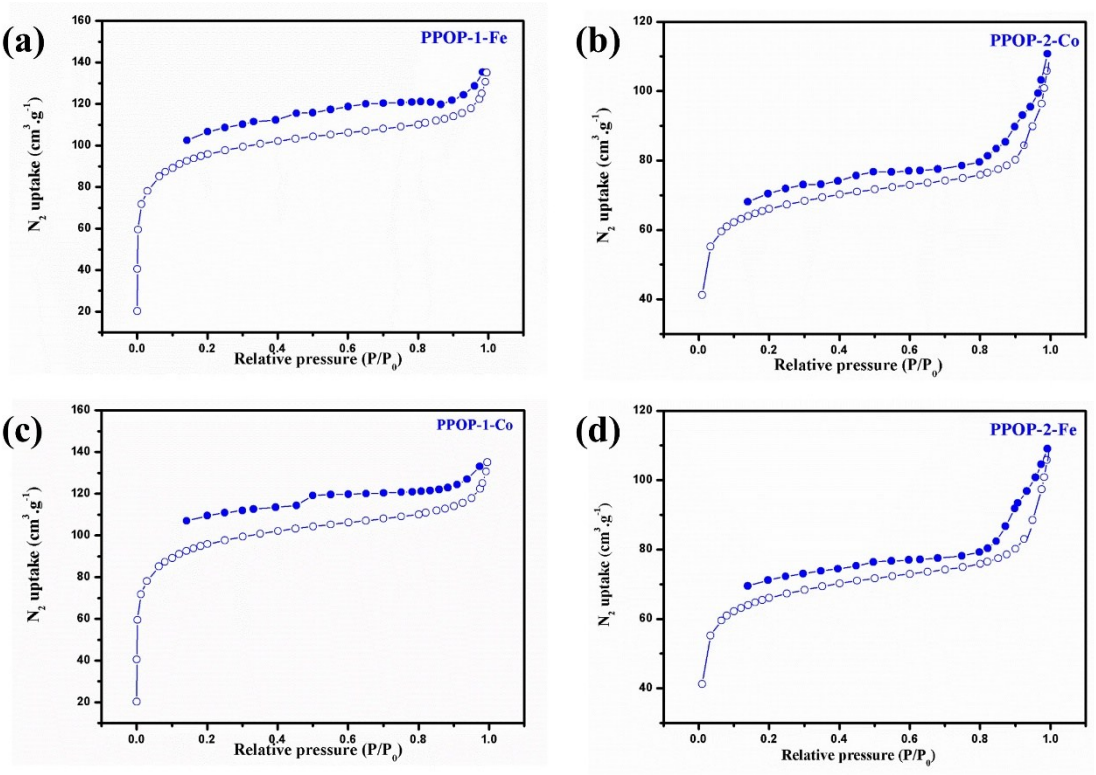

Fig. S16 N_2 adsorption/desorption isotherms of (a) **PCOF-1-Fe**, (b) **PCOF-2-Co**, (c) **PCOF-1-Co** and (d) **PCOF-2-Fe**.

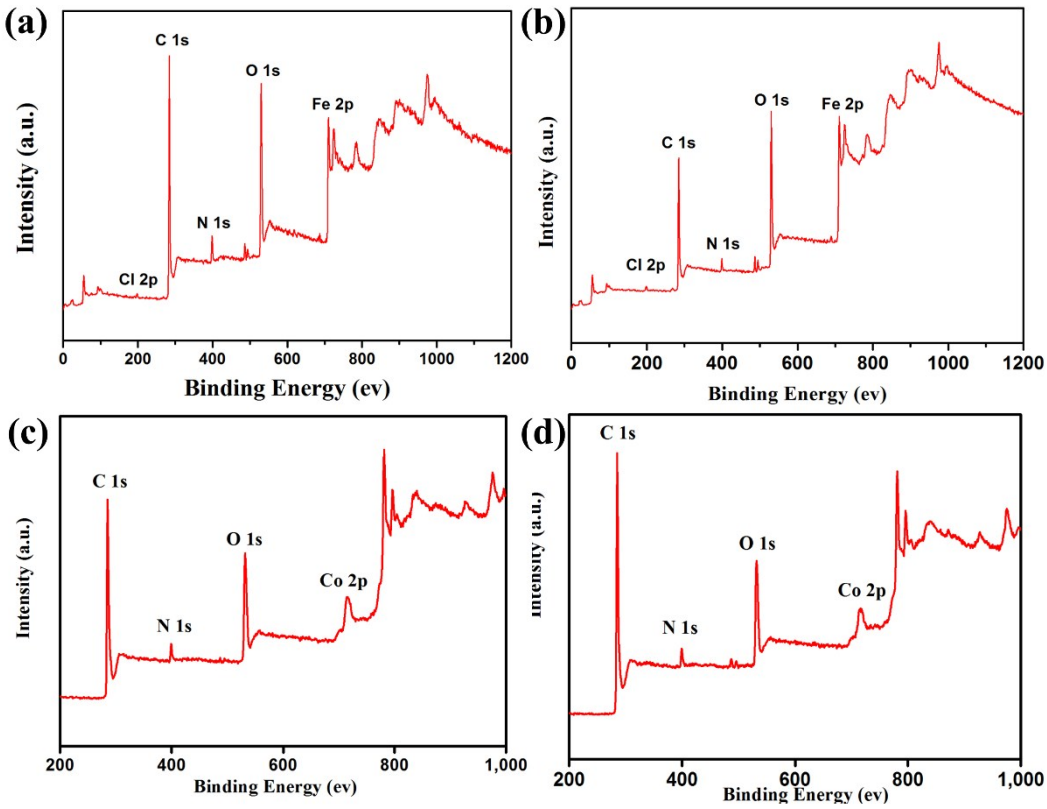

Fig. S17 XPS survey scan of (a) **PCOF-1-Fe** and (b) **PCOF-2-Fe** (c) **PCOF-1-Co** and (d) **PCOF-2-Co.**

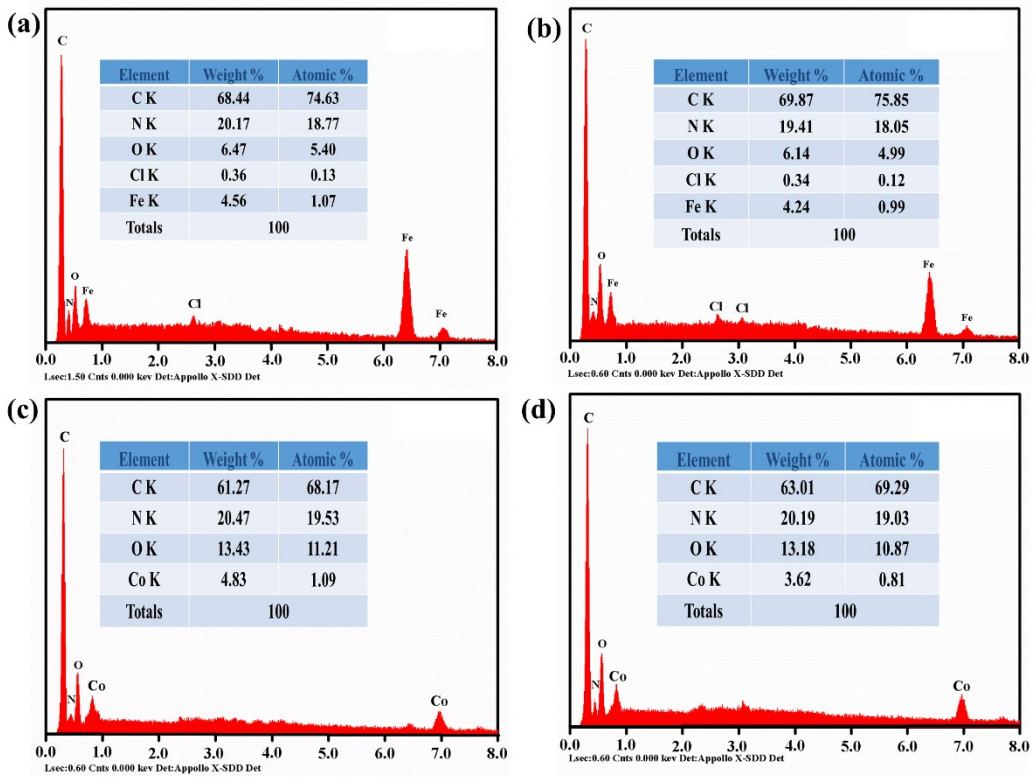

Fig. S18 Energy dispersive X-ray Spectroscopy (EDX) spectrum of (a) **PCOF-1-Fe**, (b) **PCOF-2-Fe**, (c) **PCOF-1-Co** and (d) **PCOF-2-Co**.

7. The stability of PCOF-1 and PCOF-2

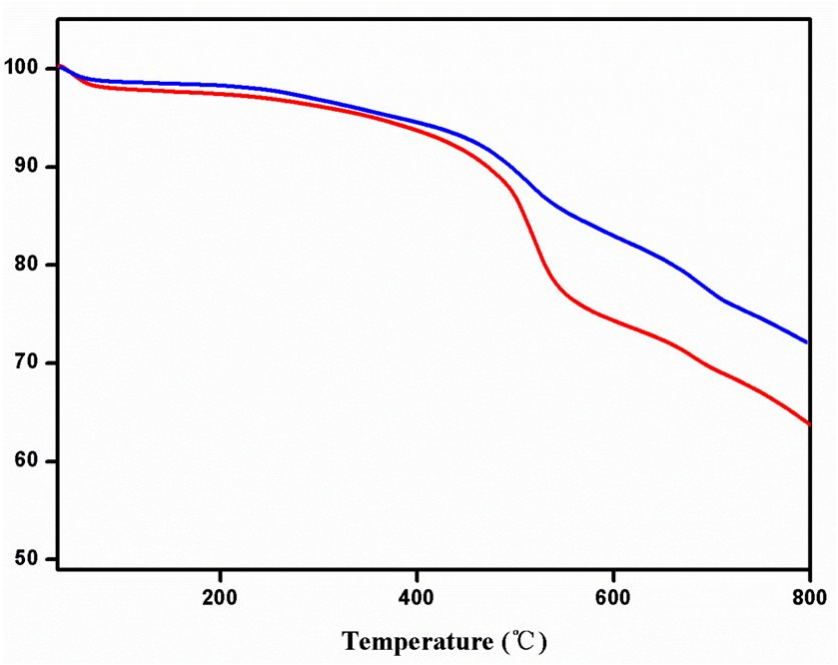

Fig. S19 TGA profiles of **PCOF-1** (red) and **PCOF-2** (blue).

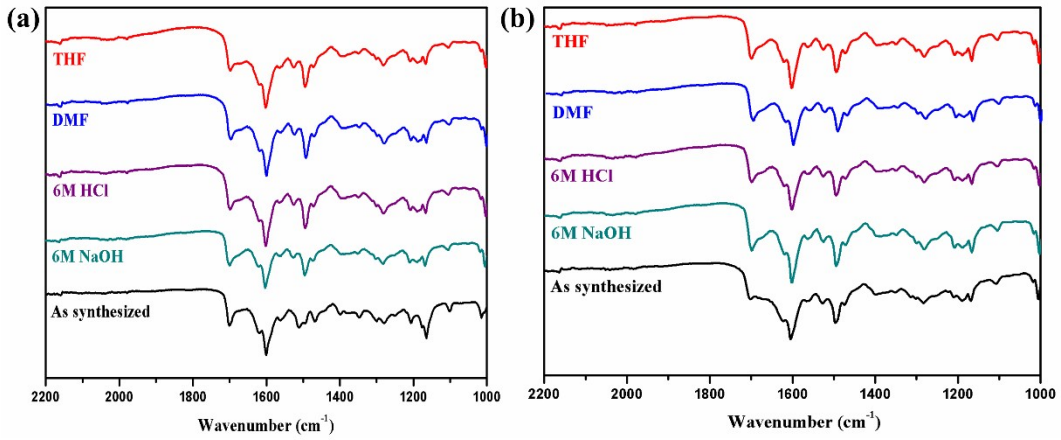

Fig. S20 FT-IR spectra of (a) **PCOF-1** and (b) **PCOF-2** after treatment for 7 days in THF (red), DMF (blue), 6 M HCl solution (purple) and 6 M NaOH solution (green).

8. Biomimetic catalysis characterization.

The mixture of the substrates with specific concentrations and H_2O_2 in 3 mL of buffer solution was catalyzed by **PCOF-1-Fe, PCOF-2-Fe** and Fe-TAPP. The products were confirmed by scanning the UV-vis absorbance on spectrophotometer and the concentrations of products were calculated by their molar extinction coefficients at respective wavelengths (for ABTS•$^+$, the peroxidized product of ABTS, is 12000 $M^{-1}cm^{-1}$ at 660 nm; for oxidized state 3,3,5,5-tetramethylbenzidine is 35800 M^{-1} cm^{-1} at 650 nm).

For kinetic study of the single substrate reaction, we propose the reactions catalyzed by **PCOF-1-Fe**, **PCOF-2-Fe** and Fe-TAPP follow widely-accepted ping-pong mechanism.[9]

$$E + S \leftrightarrow ES \overset{k_{cat}}{\rightarrow} E + P$$

Where E is the catalyst and S is the substrate. ES is the state of intermediate. P is the product, and k_{cat} is the Michaelis-Menten constant. The initial reaction rates were calculated by monitoring above wavelengths with half a minute intervals in kinetic mode. According to typical enzymatic reaction kinetic assay, the reaction rates were fitted to Michaelis-Menten equation:

$$v = v_{max} \times \frac{[s]}{(K_m + [s])}$$

where v is the initial reaction rate, v_{max} is the maximal reaction rate, [S] is the concentration of the substrate and K_m is the Michaelis-Menten constant. Lineweaver–Burk plot was employed for illustrating kinetic data and calculate the parameters by taking the reciprocal of both sides of the Michael-Menten equation.

$$\frac{1}{v} = \frac{K_m}{v_{max}[s]} + \frac{1}{v_{max}}$$

The oxidation of 2,2'-azinodi(3-ethylbenzothiazoline)-6-sulfonate (ABTS) to ABTS•$^+$ (660 nm) we referred to the previous work,[10] a series of concentrations of substrate varied from 2 mM to 10 mM along with a fixed amount of **PCOF-1-Fe**, **PCOF-2-Fe** and Fe-TAPP catalyst (ca. 40 ug) and hydrogen peroxide concentration (40 mM) in 3 mL of 4-(2-hydroxyethyl)-1-piperazineethane- sulfonic acid (HEPES) buffer. Kinetic measurements were carried out in time-course mode by monitoring the absorbance change at 660 nm for ABTS•$^+$ on a Jasco V550 UV−vis spectrophotometer with 500 rpm at 25 °C. The Michaelis−Menten constant was calculated using the Michaelis−Menten curve fit. Meanwhile, we recorded the color change for the whole process, which changed from colorless to dark green in just 2 minutes.

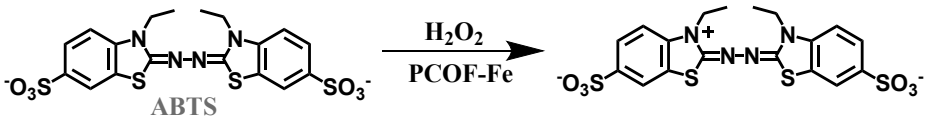

ABTS

For oxidation of 3,3,5,5-tetramethylbenzidine, acid aqueous solution (pH = 3) was selected due to the favorable reaction condition.[11] The concentrations of substrate varied from 0.2 mM to 2.0 mM along with a fixed amount of **PCOF-1-Fe, PCOF-2-Fe** and Fe-TAPP catalyst (ca. 10 ug) and hydrogen peroxide concentration of 40 mM.

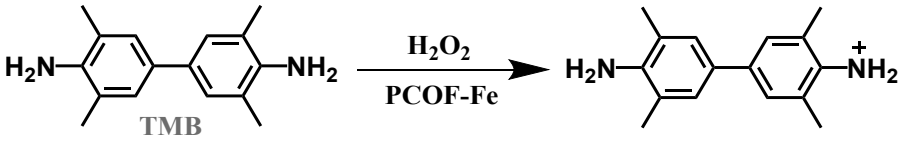

TMB

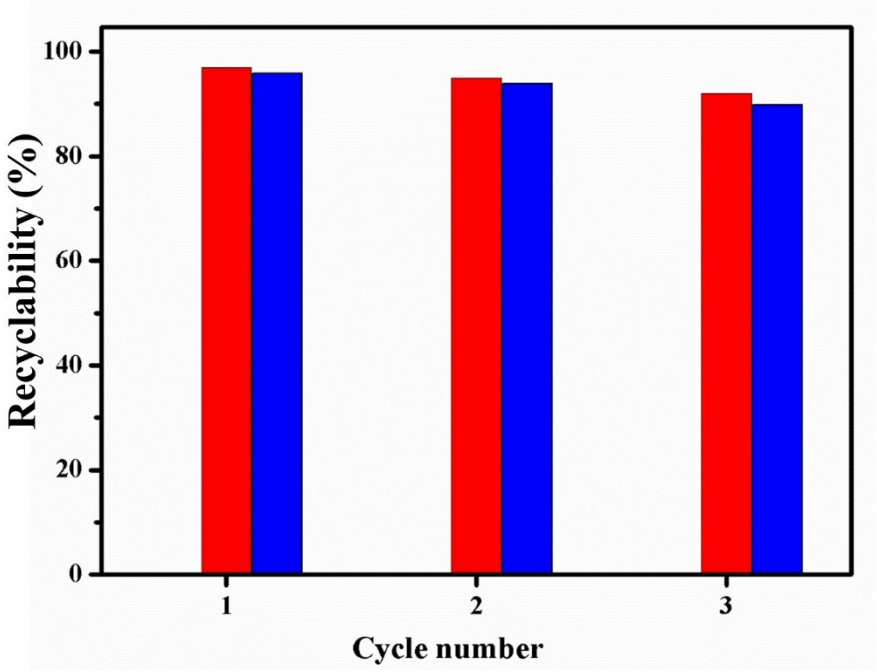

Fig. S21 Yield of catalytic recyclability studies for the oxidation of ABTS by **PCOF-1-Fe** (red) and **PCOF-2-Fe** (blue).

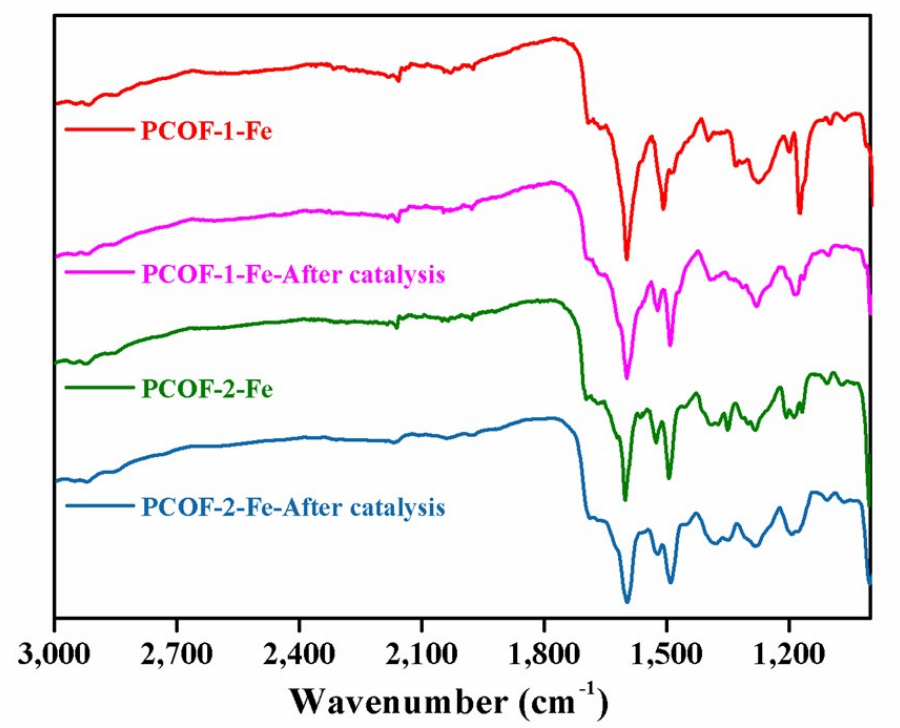

Fig. S22 The FT-IR spectra of **PCOF-Fe** before and after catalysis.

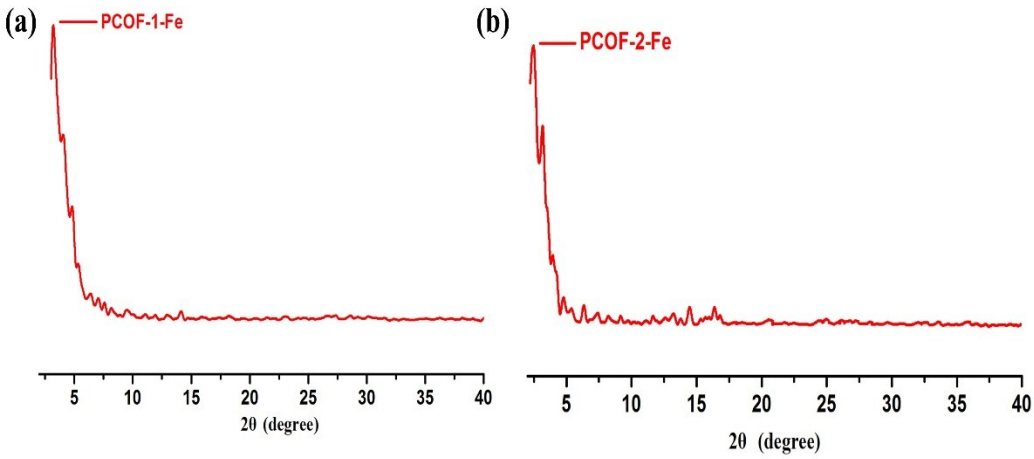

Fig. S23 PXRD patterns of (a) **PCOF-1-Fe**, (b) **PCOF-2-Fe** after catalysis.

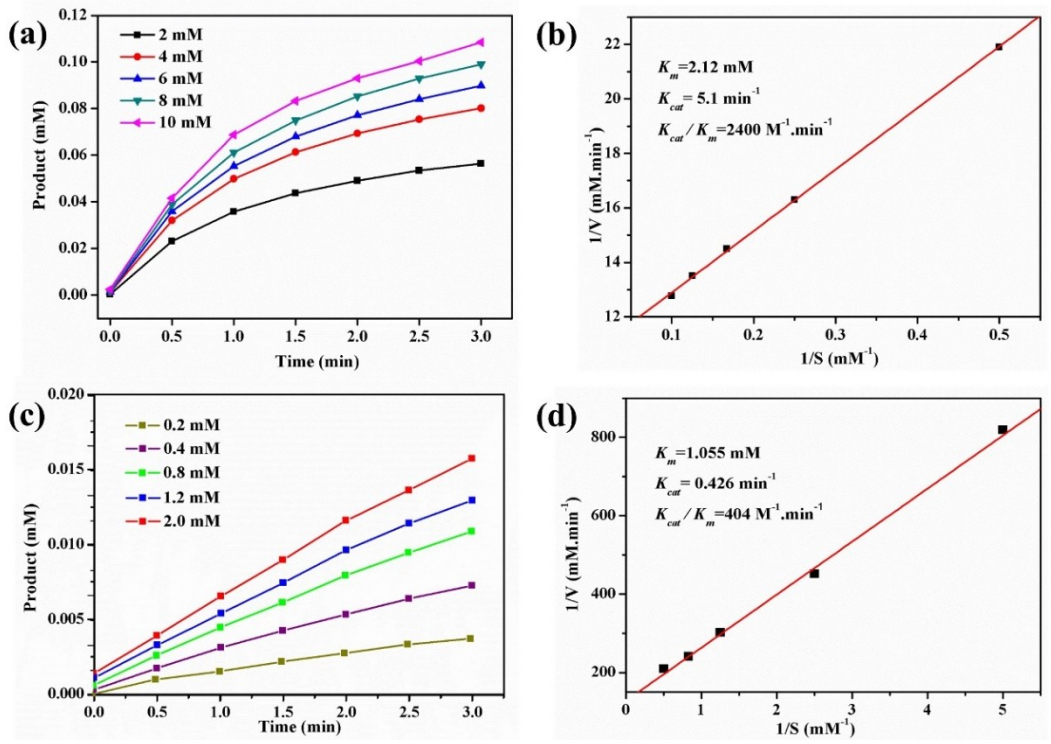

Fig. S24 (a) The fitting curves of the initial ABTS oxidation profiles at marked concentrations by Fe-TAPP; (b) The Lineweaver–Burk plots of ABTS oxidation catalyzed by Fe-TAPP; (c) The fitting curves of the initial TMB oxidation profiles at marked concentrations by Fe-TAPP; (d) The Lineweaver–Burk plots of TMB oxidation catalyzed by Fe-TAPP.

9. Electrochemical characterization

Electrochemical measurements of all samples (TAPP-Co, TABPP-Co, **PCOF-1-Co** and **PCOF-2-Co**) were performed under the same test conditions.[12] Catalytic behavior of the working electrode was measured by a CHI 760E electrochemical workstation. Electrochemical activities of **PCOF-Co** catalyst toward OER was investigated in 1 (M) KOH solution. The electrochemical catalytic activity of **PCOF-Co** was extensively studied using a three-electrode system with glassy carbon (0.07 cm^2) as the working electrode, a platinum plate and Hg/HgO were used as the counter electrode and reference electrode respectivelyBefore collecting the data, the catalysts should be run for several times. Typically, 9 mg electrocatalyst powder were spread in 1 mL of 2:3 (V/V) DI water/EtOH mix solvent with 50 μL Nafion solution. The mixture was sonicated in an ultrasonic water bath for about 1 hour to form a homogeneous catalyst ink. And the 5μL of the ink was attached on the glassy carbon, the mass loading is about 0.643 mg cm^{-2}, and dried in oven for 12 h. Linear sweep voltammogram (LSV) was obtained at the scan speed of 20 mV/s in 1 M KOH. Chronopotentiometric measurements were measured for the stability research at the current density of 10 mA cm^{-2} over 20 hours. Electrochemical impedance spectroscopy (EIS) was registered with 5 mV amplitude at 1.65V versus RHE, and the range is between 0.1 Hz and 10^5 Hz. The reversible hydrogen electrode potential was registered according to the equation: $E_{RHE} = E_{Hg/Hgo} + 0.098 + 0.0591 \times pH$. The overpotential was computed as: $\eta = E_{RHE} - 1.23$ V.

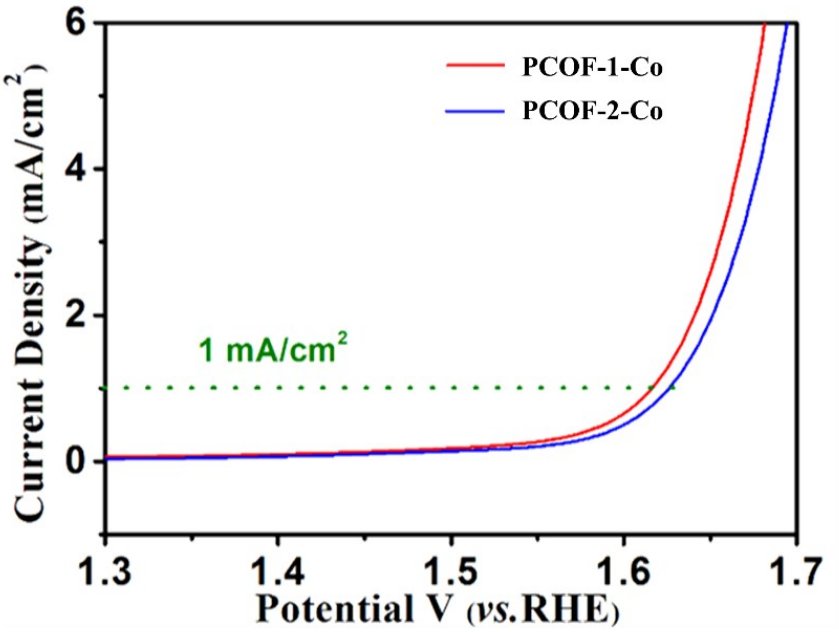

Fig. S25 LSV curves of **PCOF-1-Co** and **PCOF-2-Co** in 1.0 M KOH at 20 mV/s with *iR* compensation.

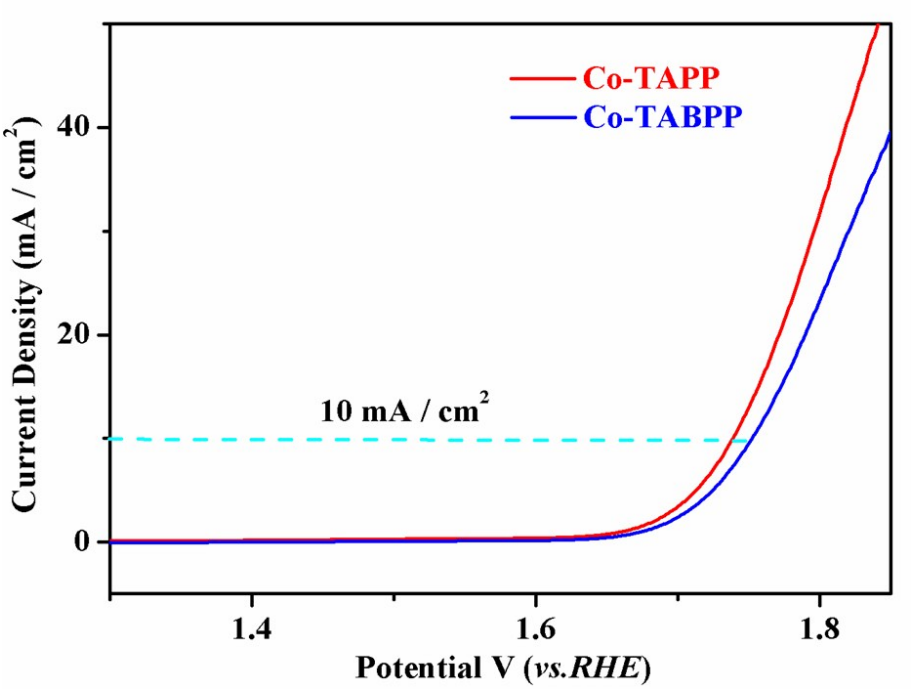

Fig. S26 LSV curves of Co-TAPP and Co-TABPP in 1.0 M KOH at 20 mV/s with *iR* compensation.

10.Crystallographic data for TFBM and MC

Table S3 Summary of crystallographic data for TFBM.

TFBM	
Formula	$C_{46}H_{38}O_4$
Fw	654.76
T (K)	173
λ (Å)	0.71073
Crystal system	tetragonal
Space group	$P4_32_12$ (No.96)
a (Å)	17.0286(10)
b (Å)	17.0286(10)
c (Å)	12.7776(15)
α (^{0})	90
β (^{0})	90
γ (^{0})	90
V (Å^3)	3705.2(6)
Z	4
Dcalc (g/cm^3)	1.174
μ (mm^{-1})	0.074
F(000)	1384
θ (^{0})	2.9, 23.2
Index ranges	-18 <= h <= 13 -18 <=k <= 18 -12 <=l <= 14
Reflections collected	7883
GOF (F^2)	1.115
$R_1{}^a$,$wR_2{}^b$ (I>2σ(I))	0.0979, 0.2256
$R_1{}^a$,$wR_2{}^b$ (all data)	0.1928, 0.3318

$R_1{}^a = \Sigma||F_o| - |F_c||/\Sigma|F_o|$. $wR_2{}^b = [\Sigma w(F_o{}^2 - F_c{}^2)^2/\Sigma w(F_o{}^2)]^{1/2}$

Table S4. Selected bond lengths [Å] and angles [°] for TFBM.

		TFBM	
C1-C2	1.380(13)	C1-C2_a	1.380(13)
C1-C5	1.508(13)	C7-C22Z	1.483(17)
C2-C3	1.412(14)	C7-C22A	1.49(3)
S2-C23	1.6756(5)	C8-C26	1.551(14)
C2-C9	1.526(14)	C10-C15	1.388(18)
C3-C4	1.384(14)	C10-C16	1.48(2)
C3-C13	1.499(14)	C12-C13	1.395(15)
C4-C17	1.539(14)	C13-C14	1.383(16)
C5-C6	1.399(12)	C14-C15	1.396(17)
C6-C7	1.443(14)	C19A-C20A	1.37(8)
C6-C18	1.510(14)	C19A-C24A	1.37(8)
C7-C8	1.371(12)	C19A-C25A	1.48(7)
C5-C6	1.399(12)	C19Z-C25Z	1.49(2)

Table S5 Summary of crystallographic data for MC.

MC	
Formula	$C_{72}H_{50}N_8$
Fw	1027.20
T (K)	173
λ (Å)	0.71073
Crystal system	triclinic
Space group	*P-1* (No. 2)
a (Å)	11.0971 (7)
b (Å)	17.1236 (11)
c (Å)	18.6175 (11)
α (^{0})	94.671 (2)
β (^{0})	102.879 (2)
γ (^{0})	94.472 (2)
V (Å^3)	3420.4 (4)
Z	2
Dcalc (g/cm^3)	0.997
μ (mm^{-1})	0.059
F(000)	1076
θ (^{0})	2.9, 25.0
Index ranges	-13 <= h <= 13 -20 <= k <= 18 -22 <= l<= 22
Reflections collected	5958
GOF (F^2)	1.029
R_1^a,wR_2^b (I>2σ(I))	0.0797, 0.2135
R_1^a,wR_2^b (all data)	0.1826,0.3234

$R_1^a = \Sigma||F_o| - |F_c||/\Sigma F_o|$. $wR_2^b = [\Sigma w(F_o^2 - F_c^2)^2/\Sigma w(F_o^2)]^{1/2}$

The formula and these parameters do not include solvent.

Table S6. Selected bond lengths [Å] and angles [°] for MC

MC			
C1A-C2A	1.428(5)	C25A-C26A	1.396(6)
C1A-C10A	1.397(5)	C26A-C27	1.364(7)
C2A-C3A	1.348(6)	C28A-C29A	1.392(5)
C3A-C4A	1.430(5)	C30A-C31A	1.493(6)
C4A-C5A	1.406(5)	C31A-C36A	1.374(8)
C4A-C5A	1.406(5)	C31A-C36A	1.374(8)
C5A-C6A	1.405(5)	C31A-C32A	1.383(8)
C5A-C11A	1.487(5)	C32A-C33A	1.381(8)
C6A-C7A	1.445(5)	C33A-C34A	1.371(8)
C7A-C8A	1.340(5)	C34A-C35A	1.362(9)
C8A-C9A	1.446(5)	C35A-C36A	1.394(8)
C9A-C10A	1.399(5)	N1B-C4B	1.369(5)
C10A-C24A	1.500(5)	N1B-C1B	1.381(4)
C11A-C12A	1.381(6)	N2B-C6B	1.379(5)
C12A-C13A	1.385(6)	N2B-C9B	1.383(4)
C13A-C14A	1.367(6)	N3B-C14B	1.424(5)
C15A-C16A	1.388(5)	N3B-C17B	1.244(6)
C17A-C18A	1.470(6)	N4B-C27B	1.424(5)

11. The fractional atomic coordinates of PCOF-1 and PCOF-2

Table S7. PCOF-1 staggered stacking

Space group Pmc_{21} Cell parameters a = 50.6034 Å b = 26.7054 Å c = 26.6992 Å $\alpha = \beta = \gamma = 90.0°$			
Atom	*x/a*	*y/b*	*z/c*
C1	0.41468	0.53415	0.65579
C2	0.39614	0.5344	0.69452
C3	0.08495	0.77901	0.48092
C4	0.10311	0.73968	0.48449
C5	0.42936	0.38323	0.18064
C6	0.41083	0.38309	0.21942
C7	0.07	-0.0841	1.04479
C8	0.08853	-0.12277	1.04374
C9	0.44401	0.57109	0.55882
C10	0.45213	0.5739	0.60919
C11	0.43149	0.57525	0.64876
C12	0.39414	0.5755	0.72669
N13	0.37601	0.57322	0.76781
C14	0.58226	0.57088	0.54433
C15	0.97883	0.18543	0.01611
C16	0.98647	0.2352	0.01638
C17	0.93165	0.20977	0.02142
C18	0.89517	0.28874	0.02868
N19	0.87802	0.33116	0.03273
C20	0.04785	0.17028	0.01692
C21	0.41566	0.60153	0.37884
C22	0.3974	0.60018	0.33957
C23	0.08576	1.0548	0.46435
C24	0.42871	0.48361	0.85984

C25	0.41048	0.48489	0.82063
C26	0.0703	0.2378	0.06562
C27	0.08844	0.27702	0.06916
C28	0.44401	0.566	0.47874
C29	0.45214	0.56206	0.42849
C30	0.43153	0.55971	0.38895
C31	0.39483	0.55692	0.31004
N32	0.37776	0.55539	0.26732
C33	0.58226	0.56746	0.49309
C34	0.97882	-0.02526	1.00268
C35	0.98647	-0.07465	0.99654
C36	0.93158	-0.05003	1.00501
C37	0.89421	-0.12791	1.00283
N38	0.87583	0.83139	0.99981
C39	0.04786	-0.01033	1.00543
N40	0.96023	0.08006	0.00997
N41	0.46029	0.5682	0.51881
C42	0.47882	0.57445	0.62433
C43	0.48647	0.57467	0.6741
C44	0.47882	0.56062	0.41339
C45	0.48647	0.55836	0.36367
C46	0.05601	0.88003	0.51451
C47	0.08222	0.89461	0.51694
C48	0.05601	0.96009	0.50941
C49	0.08222	0.94588	0.51369
C50	0.65299	0.41053	0.70763
C51	0.65163	0.45256	0.67627
C52	0.66847	0.36952	0.69348
C53	0.68231	0.37028	0.64814
C54	0.66539	0.45335	0.63095

C55	0.68068	0.41209	0.61656
C56	0.63717	0.40764	0.75358
C57	0.69411	0.41187	0.56734
C58	0.72188	0.41453	0.5646
C59	0.73463	0.41431	0.51765
C60	0.7196	0.41113	0.47329
C61	0.69179	0.4081	0.47577
C62	0.6791	0.40876	0.52289
C63	0.76398	0.41711	0.5151
C64	0.7766	0.46405	0.51149
C65	0.80443	0.46698	0.51122
C66	0.81957	0.42266	0.51419
C67	0.807	0.37561	0.51795
C68	0.77917	0.37295	0.51816
C69	0.81785	0.51621	0.50881
C70	0.83302	0.53238	0.54952
C71	0.84779	0.57973	0.54666
C72	0.84644	0.60846	0.50312
C73	0.82987	0.59074	0.4613
C74	0.81625	0.54542	0.46531
C75	0.86255	0.65373	0.49711
C76	0.67591	0.40347	0.42937
C77	0.67476	0.44306	0.39495
C78	0.65889	0.43917	0.35224
C79	0.64409	0.3956	0.34361
C80	0.6454	0.35603	0.37777
C81	0.66123	0.35989	0.42043
C82	0.62627	0.39121	0.30055
C83	0.82309	0.32953	0.52269
C84	0.82333	0.29374	0.48428

C85	0.83954	0.25146	0.4881
C86	0.85558	0.24469	0.5304
C87	0.85513	0.28018	0.56886
C88	0.83898	0.3224	0.56506
C89	0.87375	0.20219	0.53467
C90	0.73795	0.41859	0.6117
C91	0.64948	0.40621	0.52579
C92	0.73335	0.40963	0.42351
C93	0.76561	0.3232	0.52307
C94	0.76032	0.51099	0.50951
C95	0.84919	0.42543	0.51138
C96	1.10434	0.90642	0.96332
N97	0.5	0.5622	0.44425
N98	0.5	0.57409	0.59343
N99	0.	0.84546	0.51564
N100	0	0.99457	0.50618

Table S8. PCOF-2 staggered stacking

Space group Pmc_{21}			
Cell parameters a = 61.6464 Å b = 33.5150 Å c = 33.0089 Å $\alpha = \beta = \gamma = 90.0°$			
Atom	*x/a*	*y/b*	*z/c*
C1	0.37612	0.54715	0.69842
C2	0.3609	0.54839	0.72976
C3	0.07011	0.82385	0.46917
C4	0.08539	0.79311	0.47174
C5	0.39753	0.40265	0.23251
C6	0.3823	0.40135	0.26384
C7	0.05742	-0.06549	1.02442
C8	0.07277	-0.0961	1.02414
C9	0.45445	0.55877	0.53449
C10	0.46076	0.558	0.57552
C11	0.44365	0.56179	0.60716
C12	0.36393	0.57391	0.76273
N13	0.34877	0.57266	0.79557
C14	0.56628	0.56829	0.52156
C15	0.98262	0.14912	-0.00221
C16	0.98889	0.18877	-0.0027
C17	0.94385	0.16847	0.00174
C18	0.86932	0.33019	0.01302
N19	0.85596	0.36504	0.01545
C20	0.03927	0.13702	-0.00134
C21	0.37829	0.54745	0.30047
C22	0.36465	0.54949	0.2666
C23	0.07056	1.04261	0.45937
C24	0.40955	0.45439	0.75618
C25	0.39597	0.45284	0.72247

C26	0.05776	0.19154	0.03697
C27	0.07302	0.22218	0.03951
C28	0.45449	0.55154	0.46991
C29	0.46094	0.54145	0.43024
C30	0.40088	0.54578	0.29545
C31	0.37353	0.5495	0.22739
N32	0.36023	0.55093	0.19195
C33	0.56623	0.56378	0.48019
C34	0.98262	-0.01901	0.98976
C35	0.98889	-0.05843	0.98533
C36	0.94383	-0.03867	0.99197
C37	0.86816	-0.19906	0.98844
N38	0.85384	0.76737	0.98592
C39	0.03928	-0.00707	0.99184
N40	0.96738	0.06502	-0.00571
N41	0.4673	0.54874	0.503
C42	0.48258	0.55399	0.58782
C43	0.48887	0.54931	0.6278
C44	0.48262	0.53166	0.4208
C45	0.48889	0.51459	0.38445
C46	0.04595	0.90312	0.49749
C47	0.06746	0.91473	0.49982
C48	0.04595	0.96698	0.49447
C49	0.06746	0.95561	0.4979
C50	0.67217	0.43701	0.65387
C51	0.66557	0.46028	0.62084
C52	0.69034	0.41232	0.65014
C53	0.70155	0.41024	0.61334
C54	0.67693	0.45858	0.58432
C55	0.69487	0.43319	0.58

C56	0.65975	0.43711	0.69173
C57	0.70621	0.42983	0.54025
C58	0.72902	0.43368	0.53792
C59	0.73972	0.43004	0.50035
C60	0.72768	0.42342	0.46471
C61	0.7049	0.41988	0.46648
C62	0.69424	0.42261	0.50433
C63	0.76383	0.43253	0.49852
C64	0.77414	0.46997	0.4956
C65	0.79698	0.47242	0.4956
C66	0.80946	0.43716	0.49798
C67	0.79919	0.39961	0.50088
C68	0.77635	0.39742	0.5011
C69	0.80794	0.51173	0.49398
C70	0.8203	0.52448	0.52708
C71	0.83216	0.56252	0.52529
C72	0.83091	0.58582	0.49036
C73	0.81747	0.57176	0.45629
C74	0.80652	0.53537	0.45906
C75	0.84357	0.62266	0.48627
C76	0.69211	0.41414	0.4288
C77	0.69244	0.44332	0.39838
C78	0.67937	0.43925	0.36403
C79	0.66577	0.40596	0.35982
C80	0.66559	0.37662	0.3899
C81	0.67873	0.38059	0.42417
C82	0.6508	0.40233	0.32552
C83	0.8124	0.36284	0.50436
C84	0.8121	0.33411	0.4735
C85	0.82509	0.30003	0.47647

C86	0.83846	0.29441	0.51038
C87	0.83864	0.32295	0.54125
C88	0.82568	0.35701	0.5383
C89	0.8528	0.25972	0.5139
C90	0.74207	0.44272	0.57522
C91	0.67004	0.41765	0.50626
C92	0.7393	0.41921	0.42496
C93	0.76526	0.35776	0.5054
C94	0.76071	0.50728	0.49364
C95	0.83377	0.43948	0.49578
C96	1.08593	0.9267	0.95913
C97	0.41561	0.54518	0.33068
C98	0.43612	0.56282	0.32751
C99	0.40962	0.52682	0.36723
C100	0.44483	0.543	0.39643
C101	0.39471	0.57132	0.69961
C102	0.41135	0.56852	0.66734
C103	0.42905	0.59488	0.66668
C104	0.44502	0.59162	0.63683
C105	0.42598	0.53545	0.60767
C106	0.40999	0.53881	0.63746
C107	0.08715	0.10049	0.49144
C108	0.1029	0.13391	0.49073
C109	0.10361	0.16145	0.52275
C110	0.11791	0.19371	0.52166
C111	0.13131	0.17157	0.45659
C112	0.11697	0.13925	0.45769
C113	0.08695	0.76963	0.50689
C114	0.10249	0.73595	0.5092
C115	0.10374	0.71248	0.54436

C116	0.1177	0.67973	0.54621
C117	0.12969	0.69329	0.47782
C118	0.1157	0.7261	0.47599
C119	0.54953	0.56198	0.36005
C120	0.57582	0.52556	0.39981
N121	0.5	0.54147	0.44364
N122	0.5	0.5565	0.56305
N123	0	0.87549	0.49786
N124	0	0.99453	0.49225

Reference

1 *SAINT-Plus*, version 6.02; Bruker Analytical X-ray System: Madison, WI, 1999.

2 G. M. Sheldrick, *SADABS An empirical absorption correction program*, Bruker Analytical X-ray Systems: Madison, WI, 1996.

3 G. Sheldrick, *Acta Crystallogr., Sect. C: Struct. Chem.,* 2015, **71**, 3–8.

4 P. van der Sluis and A. L. Spek, *Acta Crystallogr., Sect. A: Found. Crystallogr.,* 1990, **46**, 194-201.

5 A. Spek, *Acta Crystallogr., Sect. D: Biol. Crystallogr.,* 2009, **65**, 148-155.

6 J. N. Moorthy, P. Venkatakrishnan, P. Natarajan, Z. H. Lin and T. J. Chow, *J. Org. Chem*., 2010, **75**, 2599–2609.

7 A. Bettelheim and B. A. White, et al., *Inorg. Chem*., 1987, **26**, 1009–1017.

8 Z. D. Ding, W. Zhu, T. Li, R. Shen, Y. X. Li, Z. J. Li and Z. G. Gu, *Dalton Trans.,* 2017, **46**, 11372.

9 X.-S. Wang, M. Chrzanowski, D. Yuan, B. S. Sweeting and S. Ma, *Chem. Mater*., 2014, **26**, 1639.

10 W. Zhu, Z. D. Ding, X. Wang, T. Li, R. Shen, Y. Li, X. H. Ren, Z. J. Li and Z. G. Gu, *Polym. Chem*., 2017, **8**, 4327–4331.

11 D. Feng, Z.-Y. Gu, J.-R. Li, H.-L. Jiang, Z. Wei and H.-C. Zhou, *Angew. Chem., Int. Ed*., 2012, **51**, 10307–10310.

12 H. B. Aiyappa, J. Thote, D. B. Shinde, R. Banerjee and S. Kurungot, *Chem. Mater*., 2016, **28**, 4375–4379.